Transportation Engineering 12 (2023) 100176

Contents lists available at ScienceDirect

Transportation Engineering

journal homepage: www.sciencedirect.com/journal/transportation-engineering

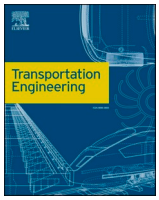

Near-field vibrations in railway track on soft subgrades for semi high-speed trains

K.S. Beena [a], M.N. Sandeep [a], Buddhima Indraratna [b,*], Rakesh Sai Malisetty [b]

[a] Division of Civil Engineering, School of Engineering, Cochin University of Science and Technology, Kochi, Kerala, India
[b] Transport Research Centre, University of Technology Sydney, NSW, Australia

ARTICLE INFO

Keywords:
Rayleigh wave
Ground vibration
High-speed railway
Peak particle velocity

ABSTRACT

For the development of a high-speed rail network in urbanised areas, ground vibration and associated damage to surrounding structures are major concerns. The problem becomes critical especially in areas with soft soil deposits due to amplification of vibration during Rayleigh wave propagation. In the present study, near field ground vibrations from a high-speed rail ballasted track are predicted for an area which contains predominantly soft marine clay deposits. A two-dimensional finite element model coupled with infinite boundaries is developed in ABAQUS. Using the finite element model, the vibration in terms of peak particle velocity (PPV) and root mean square (RMS) velocity is determined for different train speeds and soil profiles, at varying distances from the track centre. Different soil profiles are considered in this study by varying the thickness and depth of the soft clay layer. From the results, it was observed that maximum ground vibration happens when the train speed is close to the Rayleigh velocity of the soft clay layer. Further, the safe limits for residential and sensitive structures are determined for different conditions based on peak particle velocity. Considering human discomfort during vibration propagation, the vibration level in decibel scale is determined for different track configurations.

1. Introduction

High-speed rail (HSR) has become the new mode of transport system which can cater the need for lesser travel time and higher mobility of people and goods. In the environmental impact assessment of HSR projects in the urbanised areas, one of the major challenges identified is the associated ground vibration from the track structure in the nearby areas and this is especially true in regions with soft soil deposits.

Several field studies conducted using high speed trains [1,2] reported that the maximum dynamic response for the track structure is observed at a critical train speed based on the Rayleigh wave (R-wave) velocity of the ground and the resultant track vibrations are higher especially in sites having soft clay layers. Degrande and Schillemans [3] conducted field tests in Thalys track to investigate free field vibrations from HSR in the nearby area and created a standard data set for validation for further parametric studies. Zhai et al. [4,5] conducted field studies to investigate the ground vibrations induced by high-speed trains on ballastless tracks and identified that the first dominant frequency of the ground accelerations is induced by wheel base of the bogie. Nimbalkar and Indraratna [6] investigated the reduction in track deformations at high speeds by including shock mats in critical sections in the track. Furthermore, large scale laboratory investigations conducted by Indraratna et al. [7,8] proved that inclusions in the form of geosynthetics and shock mats alleviate the impacts of high-speed trains and reduce particle breakage of ballast.

Krylov [9] and Auresch [10] developed analytical models to predict ground-borne and building vibration due to HSR, while Ouakka et al. [11] proposed different vibration mitigation measures using enhanced superstructure system and protection barriers. Najibi and Jing [12] analysed the 2D transient propagation of shear waves in an infinite hollow cylinder using the graded finite element method. Also, numerical modelling studies for railway tracks were conducted to investigate ground vibration due to train movement [13–15].

Many previous studies deal with the dynamic behaviour of track structure along the length of the track during train movement, and only limited studies have reported the lateral propagation of ground vibration due to HSR in near field areas. In this study a two-dimensional finite element method (FEM) model in ABAQUS is developed for the high-speed railway track to investigate the near-field vibrations in the lateral direction of the track upto 120 m. Because of the large dimensions of the model required for near field vibration analysis, 3D FEM modelling consumes huge computational effort and time. Moreover, field investigations showed that longitudinal strains in the railway track

* Corresponding author.
E-mail address: buddhima.indraratna@uts.edu.au (B. Indraratna).

https://doi.org/10.1016/j.treng.2023.100176
Received 12 November 2022; Received in revised form 3 March 2023; Accepted 27 March 2023
Available online 30 March 2023

List of notations

V_R –	Rayleigh wave velocity
V_s –	shear wave velocity
$t(f)$ –	time of flight
$\Phi(f)$ –	phase difference
f –	frequency
d –	distance between receivers
α_z –	impedance contrast
R–	reflection coefficient
T –	transmission coefficient
ρ –	density
V_{dB} –	vibration level in decibel scale
V_{rms} –	root mean square velocity
V_{ref} –	reference velocity

are negligible when compared to that of lateral strains [6], hence approaching the condition of plane strain warrants the suitability of 2D modelling. Various past studies [13,16] have also proved that 2D numerical models can capture the ground vibration from high-speed railways in the lateral direction to a reasonable accuracy with in-situ field measurements. Detailed comparison between 2D-FEM and 3D-FEM models [17] indicates that the difference between the vertical acceleration response of rail between the two models is not significant along a straight track section. Hence for the purpose of this study, a 2D plane strain model is considered to be appropriate and adequate by taking the cross-section of the track at the sleeper location where loading is applied.

In this study, Cochin area in India is selected due to the proposed semi HSR line passing through the region where soft marine clay layer is present with different thickness underneath the top silty layer. The presence of soft marine clay deposits is a major concern due to its low R-wave velocity and the expected dynamic amplification of vibrations at critical train speeds. Further, the presence of this soft clay layer sandwiched between two stiff layers results in irregular dispersion of Rayleigh (R) waves and thus can affect near field vibrations. In the present study, the effect of embedment depth and thickness of this soft clay layer on ground vibrations due to train movement is investigated for varying train speeds. The influence of irregular dispersion of R-waves for different soil profiles on the near-field vibration response is investigated. For all the soil profiles, the R wave velocity is determined and the ground vibration in terms of peak particle velocity (PPV) is obtained at different train speeds with safe limits proposed for different types of structures.

2. Numerical simulation

A finite element model is considered in this study adopting a two-dimensional (2D) model in ABAQUS as shown in Fig. 1a. The details of the finite element model such as soil layers, model dimensions, surface nodes and infinite boundaries are shown in Fig. 1b and Fig. 1c. A full scale model is considered instead of half symmetry to eliminate the possibility of wave reflection due to the boundary condition at the axis of symmetry. The track structure is centrally placed and the subgrade model dimensions are considered as 300 m in width and 100 m in depth. The track components and the soil medium are modelled using 2D plane strain elements CPE4R, coupled with 4-node one-way infinite elements CINPE4 at the bottom and lateral boundaries. The purpose of using infinite elements is to avoid wave-reflection off the boundaries and to provide continuity, thus replicating an infinite boundary [17].

The geometry and arrangement of the track structure are fixed based on the previous studies on HSR on soft soil and also confirming to specifications for high-speed rail and embankments [18–21]. The double track consists of sleepers [2.60 m (l) x 0.24 m (h) x 0.24(w)] resting on the ballast layer at a longitudinal spacing of 0.60 m. For high-speed trains usually, standard gauge (gauge distance = 1.45 m) is used and the same is adopted in the present study.

A convergence study was conducted to arrive at the optimum mesh element size of 0.20 m, considering percentage variation for peak particle displacement and peak particle velocity. For sleepers, element size is reduced to 0.10 m due to lesser geometric dimensions and higher stress concentration. Correia et al. [13], reported that the strain level induced in the ground during wave propagation is less than the elastic strain threshold, hence linear elastic models are adopted in this study. The material properties of the track components adopted for the present model based on Indian conditions [18,22] and the range of material properties from the previous studies are summarised in Table 1 [13, 19–21]. The damping ratio adopted for the track structure including the embankment is 1% and for the subsoil it is taken as 5%. The Rayleigh damping constants are determined based on the Eigen value analysis of the track structure and ground [13,21].

2.1. Rail embankment and loading conditions

Table 2 shows the thickness of granular ballast layer based on different methods in literature [23,24] and ballast layer of 1 m thickness is adopted in this study considering the upper limit.

Considering the weak soil conditions and high flood level in Cochin area, an embankment is provided beneath the granular layer. Based on the previous studies on HSR track structure on soft clay, the height of embankment in present study is taken as 3.5 m and the geometry features of the embankment such as side slope, top width, bottom width etc. [shown in Fig. 1(a)], are based on the standard specifications for railway embankment for double lines [19,25,26]. The material properties of the embankment are given in Table 1.

For the dynamic loading on the track structure, a single bogie is considered to reduce the computational time [16]. The present study uses the five sleeper method in which the point wheel load of the train is transmitted to the adjacent five sleepers, while maximum load is on the sleeper directly below the wheel as shown in Fig. 2 [21]. The load distribution on the sleeper is modelled as load changing in time domain to simulate moving wheel load [16]. As the train speed is considered for calculating time increment in the dynamic loading model, additional dynamic amplification factor is not used. The axle load considered in the present study is 17t

The wheel load is considered as a point load with its magnitude changing in time which reaches maximum value when the wheel is directly above the considered sleeper (sleeper position $n = 3$, Fig. 2). The loading amplitude i.e., the ratio of maximum wheel load (W) transferred to the sleeper when the wheel is directly above the sleeper (0.4 W) to the load transferred when the wheel is on adjacent sleepers ($n = 1,2,$ & $4,5$) is plotted in Fig. 3 for train speeds 200, 150 and 100 kmph. It is to be noted that higher train speed is accounted by the occurrence of peak loads in shorter duration. The time increment for loading is determined as ratio of sleeper spacing (0.60 m) to the train speed and varies with train speed. Due to the overlapping effect of two adjacent wheel loads in a bogie, the shape of the loading has 'M' shape with two peaks. The loading curves for the two wheel loads from a single axle is simultaneously applied to the sleeper as shown in Fig. 1(a).

2.2. Validation of FEM model

To validate the modelling procedure, the acceleration response obtained from the numerical analysis is compared with the experimental data reported in the previous studies [13,3]. This selected case study is for a ballasted railway track at grade with Thalys high speed train (HST) travelling at 314 kmph at a site between Brussels and Paris. This field study is used for validation as it contains detailed description of all track components and soil properties needed for the FE modelling, as well as

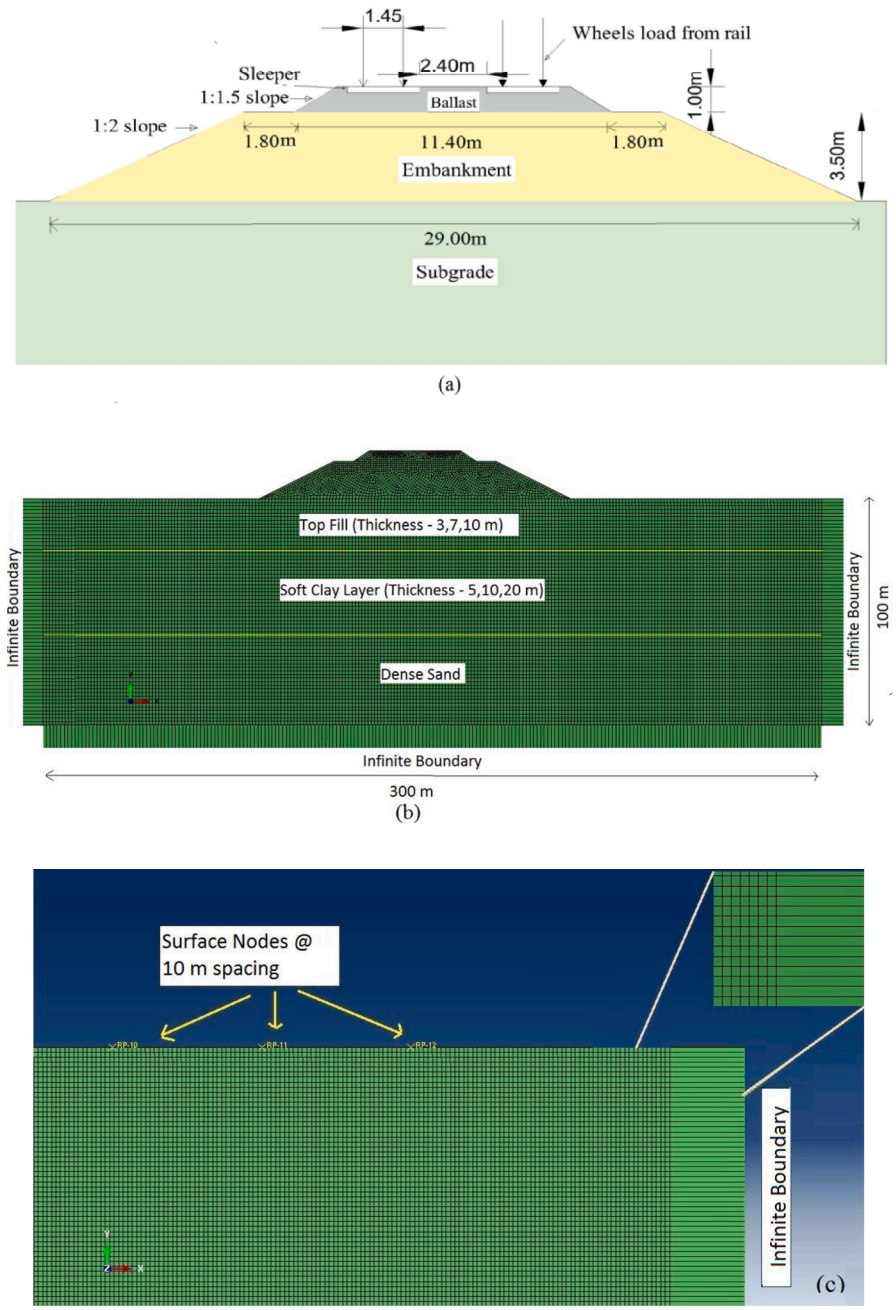

Fig. 1. (a) Schematic diagram of HST double track structure, (b) Finite element model of track structure and subsoil, (c) FEM model of track structure showing surface nodes and infinite element boundary.

field measurements for ground vibration near the track structure during the train movement. The material parameters of the Thalys HST track are given in Table 3. The soil profile in the site consists of three layers of soil with varying shear wave velocities. The loading plan was applied considering the entire train consisting of multiple bogies and a uniform axle load of 17 t for all bogies.

Fig. 4 shows the comparison of vertical acceleration obtained from the field study and the present FE analysis during the train passage for surface observation points at a distance of 4 and 24 m from the track centre on the ground. It can be seen that the developed FE model predicts the ground response in terms of peak particle acceleration with good accuracy. Confirming to field measurements, the FEM model captures the reduction of particle accelerations as distance of the observation point increased from 4 m to 24 m.

2.3. Soil characteristics in Cochin area

The numerical model is used to analyse the dynamic behaviour and related ground vibration for a general soil profile found in Cochin area, due to loading from HSR. The subsoil in Cochin area consists of top fill of silty sand typically 3 to 10 m thick, underlain by a soft marine clay layer for 10 to 20 m. Underneath the soft clay layer, medium dense sand or stiff clay layer is found extending to a depth of 40 to 60 m [27–29]. In this study, the effect of thickness and embedment depth of the clay layer is investigated on HSR induced ground vibrations near the track structure. Considering the top fill having 3 m depth, the thickness of the clay layer is varied as 5, 10 and 20 m. Also, to study the influence of the embedment depth of the clay layer, a 10 m thick soft clay layer is considered at an embedment depth (top fill thickness) of 3, 7 and 10 m. Different soil profiles with their respective notations are shown in

Table 1
Material Properties of Track Structure [13,18–22].

Track component	Parameter	Range	Present Study
Sleeper	Modulus of elasticity (kN/m^2)	$2 \times 10^7 - 4 \times 10^7$	3.8×10^7
	Density(kg/m^3)	2000 −2500	2500
	Poisson's ratio	0.15–0.20	0.15
Ballast	Modulus of elasticity (kN/m^2)	1.5×10^7–3.5×10^7	3×10^7
	Density(kg/m^3)	1600 −2300	2000
	Poisson's ratio	0.30–0.35	0.30
	Damping ratio (%)	1 - 3%	1%
Embankment	Modulus of elasticity (kN/m^2)	25,000–150,000	100,000
	Density(kg/m^3)	1800–2000	1800
	Poisson's ratio	0.30–0.40	0.30
	Damping ratio (%)	1–3%	1%

Table 2
Granular bed thickness based on different design methods [23,24].

Sl No.	Description	[24]	UIC 719R	British Rail	Maximum Value
1	Axle load(17T)	0.40m	0.70m	0.60m	0.70m
2	Cumulative tonnage (600 MGT)	0.50m	0.85m	0.70m	0.85m
3	Train speed (200 kmph)	0.35m	0.90m	0.55m	0.90m
4	Soil Condition (Resilient modulus (E-25,000 kN/m^2)	0.90m	0.95m	0.95m	0.95m

Table 4.

In this study, the elastic modulus (E) of Cochin marine clay is determined based on the shear strength values obtained from reported test results of undisturbed soil samples [28], SPT values and CPT values Sundaram et al., [29] for the soil using the average of values obtained from available correlations in literature [30–34].The Poisson ratio (μ) of the soil was estimated using the relations suggested by Kumar et al., [35] using SPT value (N).Similarly, the elastic moduli of the top fill and dense sand layer are evaluated from SPT field data using various correlations. Table 5 shows the material properties of Cochin Marine clay, top fill and dense sand used for the numerical model study. Also, the shear wave and Rayleigh wave velocities of top fill, soft clay and dense sand are determined based on the material properties [36,37] and are reported in Table 5.

3. Rayleigh wave velocity of the soil profiles

The proposed FE analysis is used to determine the R-wave velocity for each soil profile, from the vertical displacement vs time responses at selected nodes using a procedure similar to the field seismic survey method for determining the R-wave velocity of the soil profiles [38]. Each soil profile is loaded with impulse loading for a short duration of 0.05 s. Two surface observation points are selected at 50 and 60 m away from the track centre as the response very near to the track may experience distortions due to wave reflections (Fig. 1c).

Fig. 5a shows the vertical displacement response with time for soil profile 3T10S at 40, 50 and 60 m, respectively. The R-wave velocity (V_R) is determined as the ratio of the distance between observation points and the time of flight of the R- wave at each observation point.

In this study, time of flight is determined using two approaches: based on peak positive particle displacement in vertical direction (see Fig. 5a) [36,39] and based on cross correlation function in MATLAB. The time of fight values for R waves computed using two approaches are found to be similar as shown in Table 6. Fig. 5b shows the retrograde elliptical movement during R-wave propagation at 40, 50 and 60 m from the centre of the track. Because of R-wave propagation [39], the particles at observation points move in lateral direction, i.e., parallel to

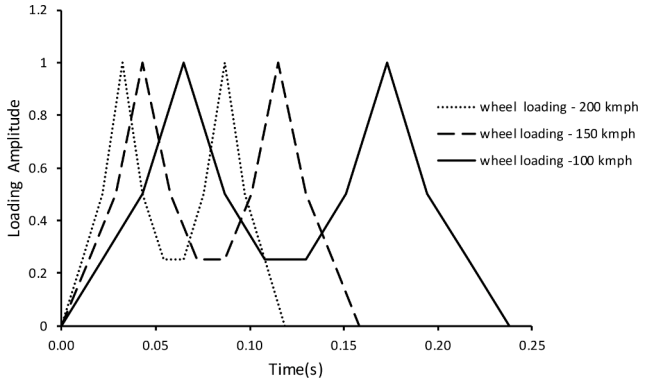

Fig. 3. Load time distribution for a single bogie.

Table 3
Material properties used for model validation [13,3].

Description	Modulus of Elasticity (MPa)	Density (kg/m^3)	Poisson's ratio	Damping ratio
Sleeper	30,000	2054	0.20	
Ballast	200	1800	0.10	0.01
Subballast	300	2200	0.20	0.01
Capping Layer	400	2200	0.20	0.01
Soil 1	48	1850	0.30	0.03
Soil 2	85	1850	0.30	0.03
Soil 3	250	1850	0.30	0.03

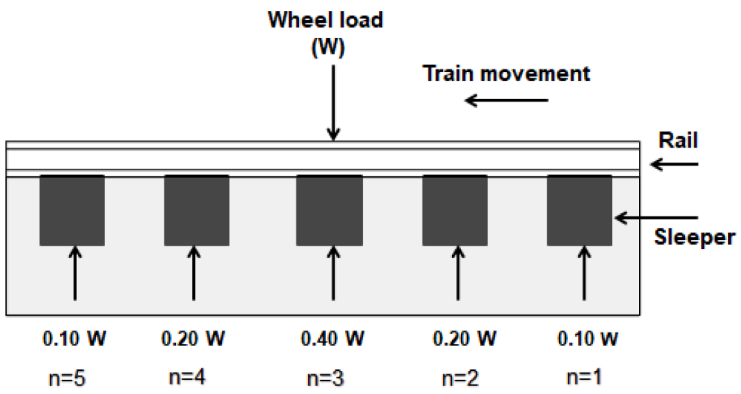

Fig. 2. Load transfer by five adjacent sleeper method [21].

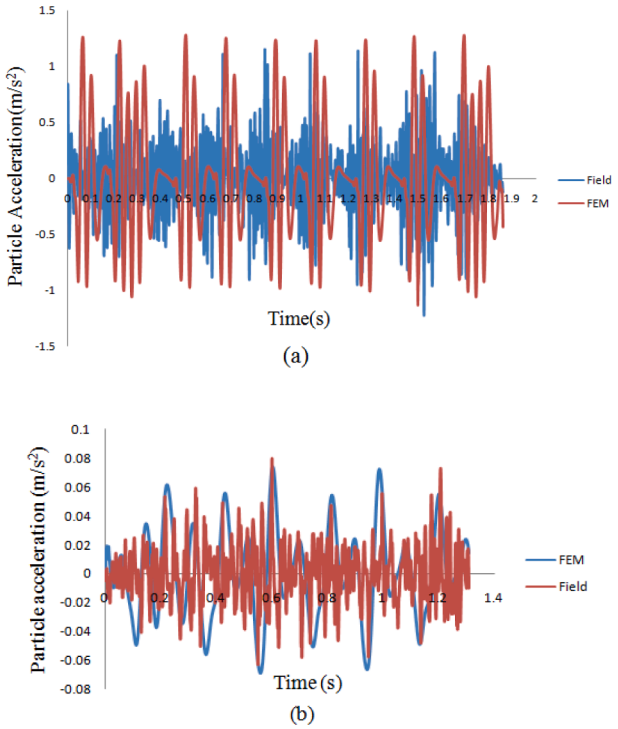

Fig. 4. Comparison of field and FEM responses at (a) 4 m and(b) 24 m from the track centre for Thalys Track.

Table 4
Details of soil profiles considered for study.

Soil Profiles	Top layer thickness (m)	Soft clay layer thickness(m)	Notation
1	3	5	3T5S
2	3	10	3T10S
3	3	20	3T20S
4	7	10	7T10S
5	10	10	10T10S

Table 5
Material Properties used for the present study.

Sl No	Description	Modulus of elasticity (kN/m^2)	Density (kg/m^3)	Poisson's ratio	Shear wave velocity (kmph)	Rayleigh wave velocity (kmph)
1	Top fill (Sand with fines)	25,000	1600	0.35	273.86	250.47
2	Soft Cochin Marine Clay	3500	1450	0.25	111.86	100.64
3	Dense sand	58,000	1900	0.40	375.89	346.19

direction of wave propagation in addition to vertical direction as observed from Fig. 5b. It can also be observed that as distance from the track increases, the particle displacements in the vertical direction are attenuated due to soil damping.

The R-wave velocities computed for different soil profiles based on peak displacements are shown in Table 6 and are found to be lower for the combined profiles in comparison with the R-wave velocity of top fill, which may be due to the presence of soft clay layer having a low R wave velocity as shown in Table 5. The R-wave velocities of the combined soil profiles in this study ranges from 171.40 kmph to 225 kmph for different clay layer thicknesses and embedment depths. It can be noted from Table 6 that the embedment depth of the clay layer is more detrimental than the thickness of the clay layer for R-wave velocities. Also, the R-wave velocity of the soil profile increases with increase in the embedment depth of the clay layer.

3.1. Dispersive property of R- waves in layered media

In layered medium the R wave is dispersive and the soil profiles considered in this study are irregular dispersive or inversely dispersive due to the presence of soft clay layer in between two stiff layers [40]. For these profiles, the R-wave velocity varies irregularly with depth, due to the presensce of softer layer in between the stiffer layers. Dispersion curves are used to study the variation of wave velocity with frequency. To find the dispersion curve, the displacement vs time responses from the FE analysis at various distances from the track centre is converted to the frequency domain using Seismo Signal software. The time of flight $t(f)$ is found out using phase difference $\Phi(f)$ between two signals determined for each frequency as follows [41].

$$t(f) = \Phi(f)/2\pi f \quad (1)$$

where,$\Phi(f)$=phase difference for a given frequency in radians, f=frequency in cycles per seconds(cps)

The velocity of R-wave is determined as:

$$V_R = d/t(f) \quad (2)$$

where, d = distance between receivers.

As the phase difference $\Phi(f)$ is also a function of the frequency(f), the dispersive equation for R-wave velocity cannot be explicitly interpreted as linear relationship Luna and Jadi, [41]. The calculation of V_R is performed for each frequency, and the results for different soil profiles are plotted in the form of a dispersion curve as shown in Fig. 5c. It may be noted that, at lower frequency, the R-waves have longer wavelength, and the waves penetrate more into the soil profile. Conversely at high frequencies, the depth of penetration of R-wave is small due to smaller wavelength. As seen in Fig. 5c, for the soil profiles analysed, the R-wave velocity is low when the soft clay layer is located at shallow embedment depths (3T5S, 3T10S, 3T20S) when compared to that of higher embedment depths (7T10S and 10T10S). This is due to the relative low R-wave velocity of the soft clay layer when compared to that of the top fill and dense sand layers and at lower frequencies the R-waves mainly propagate in the soft clay layer for the profiles 3T5S, 3T10S, and 3T20S. Further, the frequency corresponding to R-wave velocity for 3T5S is higher indicating a shorter depth of penetration due to lower clay layer thickness. For profiles 3T10S and 3T20S, the higher thickness of soft clay layer allows the R-wave to go deeper, thus having lower frequencies even though the R-wave velocity remains almost same. For the soil profiles 7T10S and 10T10S, the R waves are mainly confined in the stiff surface layer, resulting in higher R-wave velocity when compared to the soil profiles with shallow embedment depth of soft lay layer.

4. Parametric study

The effect of soil layering on the vibration level due to HSR can be explained using impedance properties of the soil layer interfaces. During wave propagation in the layered soil profiles, reflection and transmission of wave energy happen at the soil layer interfaces. The differences in impedance of the soil layers influence the wave propagation in the layered medium and the reflection and transmission of wave energy at the interfaces are characterised using reflection and transmission coefficients. Table 7 shows the impedance properties of the soil layer interfaces which are determined based on the soil properties given in Table 5. The soil layers having impedance contrast less than 0.4 and greater than 2 can be considered as an interface with strong impedance contrast [42]. It can be seen that due to the presence of the soft clay layer, strong impedance contrast exists for soil layer interfaces with clay layer. The impedance, impedance contrast, reflection and transmission coefficients are found using Eqs. (3)–(5) [43].

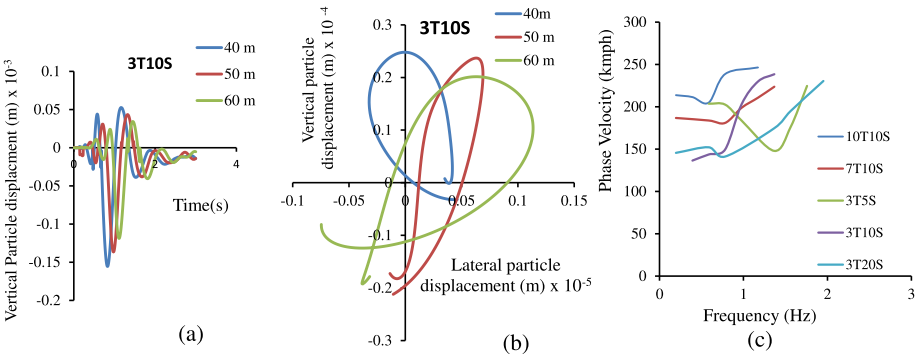

Fig. 5. (a)Vertical particle displacement vs time graph for soil profile 3T10S (b) Vertical displacement vs Lateral particle displacement during Rayleigh wave propagation for soil profile 3T10S (c) Rayleigh wave frequency dispersion curves for different soil profiles.

Table 6
Determination of R-wave velocity for different soil profiles.

Soil Profiles	Time of flight (peak displacement) (s)	Time of flight (cross correlation) (s)	R-wave velocity(kmph)
3T5S	0.195	0.190	184.61
3T10S	0.210	0.200	171.43
3T20S	0.208	0.200	173.08
7T10S	0.180	0.170	200.00
10T10S	0.160	0.150	225.00

Table 7
Impedance properties of soil layer interfaces.

Sl No	Soil Interface	Impedance contrast	Reflection coefficient	Transmission coefficient	Remarks
1	Top fill-Soft clay	2.75	−0.47	0.53	Downward propagation from surface
2	Soft clay-Dense Sand	0.22	0.64	1.64	Downward propagation from surface
3	Soft clay-Top Fill	0.36	0.47	1.47	Reflected upward propagation

$$Impedancecontrast, \quad \alpha_z = Vs_1\rho_1/Vs_2\rho_2 \tag{3}$$

$$Reflectioncoefficient, \quad R = (1-\alpha_z)/(1+\alpha_z) \tag{4}$$

$$Transmissioncoefficient, T = 2/(1+\alpha_z) \tag{5}$$

where, V_{s1}- shear wave velocity of first layer; ρ_1–density of first layer; V_{s2}- shear wave velocity of second layer; ρ_2- density of second layer.

4.1. Effect of soil profiles on the peak particle velocity

Fig. 6a shows the variation of PPV with distance from the track centre for the soil profiles 3T5S, 3T10S and 3T20S, with varying clay layer thickness for same top fill thickness at a train speed of 100 kmph. The distance of observation points from the track centre is varied from 15 m to 120 m. It can be noted that PPV decreases as distance from the track centre increases for all the soil profiles for the train speed of 100 kmph. However, undulations in the responses are observed at certain points due to reflected waves from the interface of soil layers. For soil profiles considered in the present study, reflection of waves can happen at two-layer interfaces namely top fill-soft clay and soft clay-dense sand interfaces. For both these interfaces, the impedance contrast and reflection coefficients are found to be high as shown in Table 7.

After an initial decline in PPV, two localised peaks are observed in the PPV response for the soil profiles 3T10S and3T20S (Fig.6a). The first high amplitude peak corresponds to reflected waves from the top fill–soft clay interface and the second peak corresponds to soft clay –dense sand interface respectively. For the 3T20S profile (Fig.6a), due to the increase in the embedment depth of soft clay-dense sand interface, these localized peaks in PPV- distance response occurred at larger spacing compared to soil profile 3T10S.This may be due to the larger

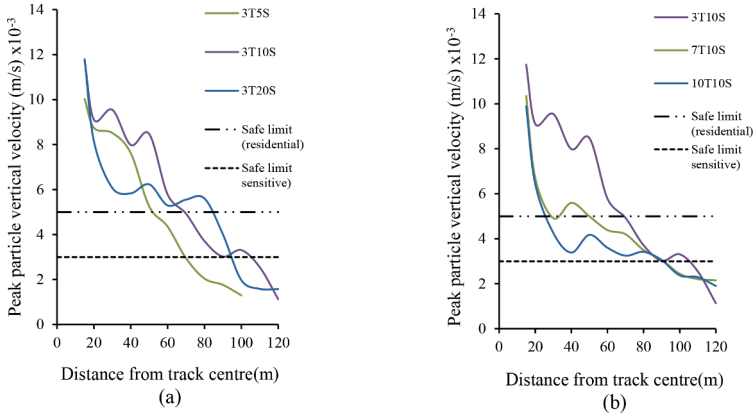

Fig. 6. Peak particle velocity for varying distance from track centre at train speed of 100kmph for soil profiles (a) varying clay layer thickness (b) varying top fill thickness.

incident angle for waves at soft clay-dense sand interface and longer wave path for the 3T20S profile (owing to its larger clay layer thickness). In contrast, the soil profile 3T5S is characterized by the absence of localized peaks. In this case, owing to the lesser layer thickness of top fill and soft clay, reflection of waves occurs from both the top fill-soft clay and soft clay-dense sand layer interfaces to the surface level. The absence of multiple peaks may be due to the superimposition of these reflected wave fronts from the soil interfaces very near to the embankment and the polarity reversal of the reflected waves from two different interfaces.

Fig. 6b shows the variation of PPV with distance from the track centre for the soil profiles 3T10S,7T10S and 10T10S, with varying embedment depth of clay layer with same thickness at a train speed of 100 kmph. For profiles 7T10S and 10T10S (Fig. 6b), due to the greater embedment of soft clay – dense sand layer interface, reflection from this interface is negligible. Also, for these soil profiles, due to the larger depth of top fill –soft clay interface, wave propagation mainly occurred in the stiff top fill and the surface vibration level is less when compared to other cases.

From all the predicted results, it is observed that the depth of top soil-clay interface has major influence on PPV. This is due to the fact that the top soil-clay interface acts as a reflective boundary and higher vibrations are observed at the surface when the interface is at shallower depths. Also, as the embedment depth of the soft clay layer increases, the wave energy reaching the interface is reduced due to damping, resulting in lower amplitude of reflected waves. Further, it can be observed that for mitigation of ground vibration in these soil profiles, infill trench method closer to the track structure may not be effective, as localised increase of ground vibration is observed away from the track structure due to wave reflection from the soil interfaces below the surface.

4.2. Effect of train speed on the peak particle velocity

To determine the effect of the train speed on ground vibration, 5 different train speeds (50, 75, 100, 150 and 200 kmph) are considered. The ground vibration in terms of particle velocity is obtained at various distances from the track centre.

Fig. 7 shows the variation of PPV with distance from the track centre for the soil profiles 3T5S, 3T10S and 3T20S at different train speeds where the embedment depth is kept constant with different clay layer thickness. The influence of different embedment depths of soft clay (soil profiles:7T10S and 10T10S) on the variation of PPV with distance from the track centre is shown in Fig. 8. For all the soil profiles considered in this study, it can be noted that PPV values are higher for lower train speeds (50–100 kmph) and reduce at higher train speeds (150–200 kmph). This may be due to the dynamic amplification of ground vibration at lower train speeds matching with the lower Rayleigh velocity of the soft clay layer (V_R = 100.64 kmph, Table 5). At higher train speeds, the loading duration reduces for the sleeper, resulting in waves with high frequency and smaller wave lengths. As the amplitude of R-waves becomes negligible at a depth equivalent to 1–2 times of wavelengths, these waves are mainly confined to the top layer at higher train speeds (Table 5). This results in a lower level of near field vibration due to HSR. But in the case of lower train speeds, the waves have higher wave lengths and greater depth of penetration into the soft clay layer. This causes increased surface vibration due to low R-wave velocity of the soft clay layer and wave reflections at the top fill –soft clay interface. It can be noted that the R wave velocity of the soil medium is an indicative value of high ground vibration and during train loading high ground vibration happens for a range of train speeds close to the R wave velocity of the soft clay layer. Previous studies have noted that higher ground vibrations can happen at lower train speed range (50–100 kmph) when compared to higher train speeds (150–200kmph) and critical train speeds are a set of values depending upon the subsoil profile [44,45]. Higher ground vibration can be expected for the lower train speed range of 50–100 kmph for the irregular dispersive soil profiles with soft clay layer as in the case of Cochin area. This can be dangerous in regions where the train speeds are lower such as areas near to train stations and places with a change in gradient and alignment of the track.

4.3. Safe distance from the track centre

In this study, PPV and vibration in decibel scale (V_{dB}) are used to calculate the safe distance from the track centre considering damage to buildings and sensitive structures. The vibration limits (in PPV) based on German national standard DIN4150–2 [46] for commercial structures, residential structures and sensitive structures are 20, 5 and 3 mm/s, respectively. Similarly, based on Federal Transit Administration (FTA), the range of limits prescribed for commercial structures is 12.7–7.6 mm/s. For residential structures and sensitive structures, the vibration limits are 5.1 and 3 mm/s based on FTA criteria [47]. Adopting these criteria, the safe limit of PPV for residential and sensitive structures is taken as 5 and 3 mm/s, respectively.

For different soil profiles, the safe distance from the track structure based on the safe limit of PPV is determined and given in Table 8. The safe distance for soil profiles 3T10S and 3T20S is greater compared to that of other soil profiles considering residential structures. Generally, for a site having soft clay layers in Cochin area, the safe distance for residential structures can be takes as 90 m and that for sensitive structures can be taken as 120 m. Also, it can be observed that at higher train speeds, the safe limit for residential structures reduces to 40 m and for sensitive structures it reduces to 70 m. This indicates that for the considered soil profiles in Cochin area, lesser ground vibration problem can be expected at higher train speeds (150–200 kmph) even in

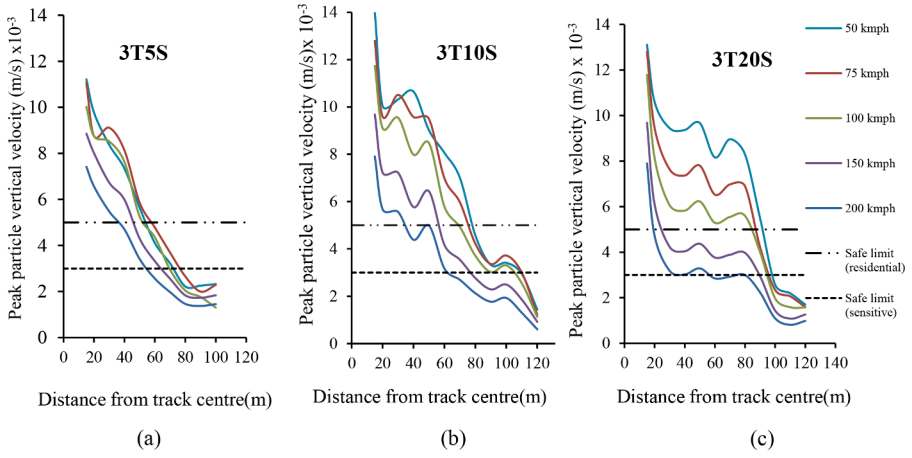

Fig. 7. Peak particle velocity for varying distance from track centre at different train speeds for soil profiles (a) 3T5S(b) 3T10S and (c) 3T20S.

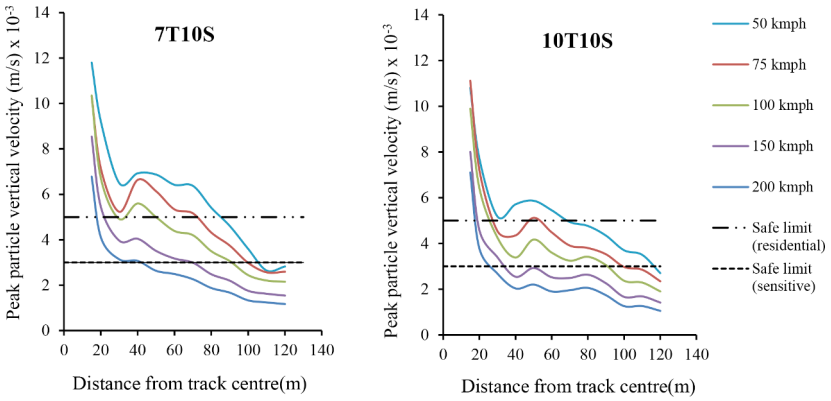

Fig. 8. Peak particle velocity for varying distance from track centre at different train speeds for soil profile (a) 7T10S and (b) 10T10S.

Table 8
Safe limits for different structures based on peak particle velocity.

Sl No	Soil Pro-File	Safe limit for residential structures(m) for low speed (50 kmph)	Safe limit for sensitive structures (m) for low speed (50 kmph)	Safe limit for residential structures(m) for high speed (200 kmph)	Safe limit for sensitive structures (m) for high speed (200 kmph)
1	3T5S	60	80	40	60
2	3T10S	90	110	40	70
3	3T20S	90	100	30	60
4	7T10S	80	120	20	50
5	10T10S	70	120	20	30

urbanized areas where existing structures are at close proximity to the track structure.

Federal Transit administration (FTA) utilises a decibel scale to assess the vibration level in ground due to different dynamic loading conditions. The vibration scale is based on root mean square (RMS) velocity. The RMS amplitude is calculated for the total duration of the signal and is used to express the magnitude of the vibration signal felt by the human body and sensitive instruments considering the fluctuations in vibrations including the effect of duration of signal [47].

The vibration velocity level in decibels can be calculated as follows

$$V_{dB} = 20log_{10}\left(V_{rms} \,/\, V_{ref}\right) \tag{6}$$

where, V_{dB}– vibration level in decibel scale; V_{rms}- RMS velocity; V_{ref}= reference velocity (which is taken as 2.54×10^{-8} m/s)

As per the FTA criteria, the vibration limit for cosmetic damages in buildings near to high-speed rail lines is 100 dB as shown in the Fig. 9. Considering human comfort, the vibration levels are limited to 80 dB for residential structures and 83 dB for public buildings. The vibration limits for structures with vibration sensitive equipment such as hospitals, research labs, concert halls, studios etc., the limit is lowered to 65 dB. The vibration level at each distance for different train speeds and soil profiles are determined based on Eq. (6). Figs. 9 and 10 shows the vibration level with distance for soil profiles 3T5S, 3T10S, 3T20S and soil profiles 7T10S and 10T10S, respectively. Based on the vibration limit of 100 dB for structural damage criteria, the safe distance for this soil profile can be fixed as 90 m. As the distance from the track centre increases the vibration level decreases for all the train speeds. Highest vibration levels are noted for train speed of 50 and 75 kmph. It can be observed that even at distance 90–100 m the vibration level is high considering human discomfort and disturbance to sensitive instruments for which the limiting values are 80 and 65 dB respectively. Similarly, for other soil profiles also vibration levels are determined. The vibration level in decibel scale at 90 m from the track centre for soil profiles 3T5S, 3T10S and 3T20S are 90.38, 94.75 and 93.27 dB respectively at a train speed of 50–75 kmph. As the embedment depth increases vibration reduces as to 89.54 and 87.54 dB for 7T10S and 10T10S soil profiles respectively.

4.4. Limitations

In this paper, the track modelling was limited to 2D finite element model for the assessment of vibration propagation in near field domain due to HSR due to computational constraints. This study only considers the lateral propagation of R-waves from the track centre due to sleeper excitation caused by a single bogie. More sophisticated models such as

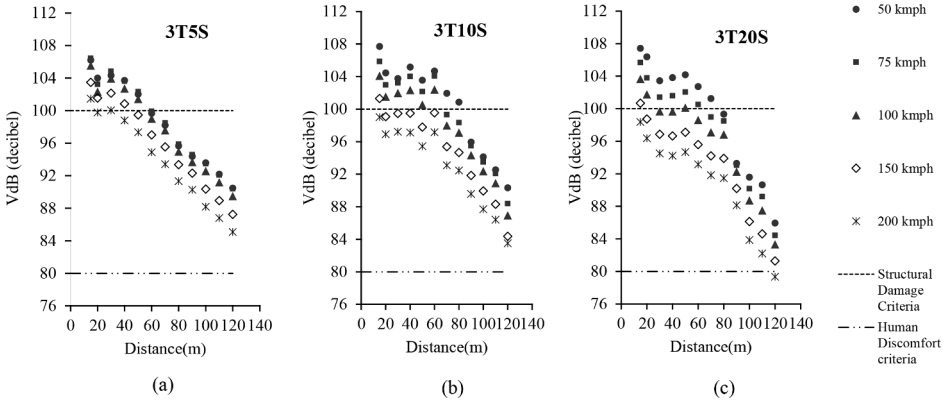

Fig. 9. Vibration in db for increasing distances from track centre at different train speeds for soil profiles (a) 3T5S(b) 3T10S and (c) 3T20S.

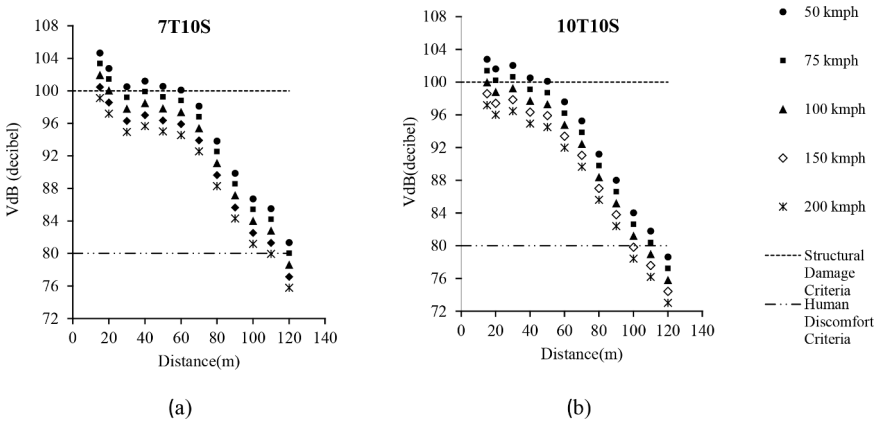

Fig. 10. Vibration in db for increasing distances from track centre at different train speeds for soil profiles (a) 7T10S and (b) 10T10S.

2.5D and 3D FEM are required to include the effects of loading by subsequent bogies on adjacent sleepers which become important at critical speeds due to the formation of Mach cones. Further, 3D FEM models are advantageous while estimating the propagation of R-waves which affect vibrations in rails and other track layers and related stress rotation [48], albeit the need for much greater computational effort and considerabley higher capacity computer facilities for large discretised mesh domains. The material model considered for the present study is a linear elastic model considering strain level within elastic threshold during wave propagation. Further investigation using non-linear models, which can predict stiffness reduction of the materials at higher strain levels and material anisotropy within the soil layers, needs to be conducted.

5. Conclusions

This study investigates the effects of soft marine clay layer and train speed on the generated ground vibration during train loading. A high-speed railway track in Cochin area is modelled using 2D Finite element method (ABAQUS) based on specifications and recommendations for HSR in the previously reported studies. Numerical simulations are carried out with different soil profiles with soft marine clay layer and the lateral safe distance for different types of structures from track centre is determined based on standard vibration criteria. The following conclusions can be made based on the results of this study:

- The presence of soft clay layer at shallow depths reduces the R-wave velocity of the ground significantly. For the soil profile having 10 m thick soft clay layer at 3 m depth, the R-wave velocity is found to be 171.43 kmph. As the depth of clay layer is increased to 7 and 10 m, the R-wave velocity increased to 200 and 225 kmph respectively.
- For irregular dispersive soil profiles with low velocity soft clay layer between two stiff layers, there will be localized increase in the PPV in areas near to the track structure during train movement due to wave reflection from soil interfaces with high impedance contrast. The most influencing factor on the ground vibration in soil profiles with soft clay layer is the depth of the top fill-soft clay interface from which wave reflections are higher.
- The ground vibration is found to be higher when the train speed is close to the R wave velocity of the soft clay for the considered soil profiles. In all the profiles with soft clay layers, the PPV values are higher for lower train speed in the range of 50–100 kmph when compared to those for higher train speed of 150–200 kmph.
- Based on PPV, the safe limits are obtained as 90 m for residential buildings and 120 m for sensitive structures for the ground profiles in Cochin area with the presence of soft clay layer.
- Considering the FTA criteria in dB for all soil profiles considered the vibration levels are less than 100 db at 90 m, which is the limit for structural damage to structures. But vibration levels are high considering structures housing sensitive instruments which necessitate the adoption of suitable mitigation measures.

Declaration of Competing Interest

The authors declare that they have no known competing financial interests or personal relationships that could have appeared to influence the work reported in this paper.

Data availability

Data will be made available on request.

Acknowledgment

This work is part of inter institutional research collaboration between Cochin University of Science and Technology, Kochi, India and the UTS Transport Research Centre, Sydney, Australia. The 1stauthor acknowledges the training obtained during the Australian Prime Minister's Endeavour scheme, and the 4th author acknowledges the training under an Australian Research Council's ITTC-Rail project.

References

[1] G. Kouroussis, D.P. Connolly, O. Verlinden, Railway-induced ground vibrations – a review of vehicle effects, Int. J. Rail Transp. 2 (2) (2014) 69–110.
[2] C. Madshus, S. Lacasse, A. Kaynia, L. Hårvik, Geodynamic challenges in high-speed railway projects, Geotech. Eng. Transp. Proj. GSP 126 (2004) 192–215.
[3] G. Degrande, L. Schillemans, Free field vibrations during the passage of a Thalys high-speed train at variable speed, J. Sound Vib. 247 (1) (2001) 131–144.
[4] W. Zhai, K. Wei, X. Song, M. Shao, Experimental investigation into ground vibrations induced by very high-speed trains on a non-ballasted track, Soil Dyn. Earthq. Eng. 72 (2015) 24–36, a.
[5] W. Zhai, P. Liu, J. Lin, et al., Experimental investigation on vibration behaviour of a CRH train at speed of 350kmph, Int. J. Rail. Transp. 3 (1) (2015) 1–16, b.
[6] S. Nimbalkar, B. Indraratna, Improved performance of ballasted rail track using geosynthetics and rubber shock mat, J. Geotech. Geoenviron. Eng. 142 (8) (2016), 04016031. –04016031.
[7] Indraratna, B., Ngo, T., Rujikiatkamjorn, C. Performance of ballast influenced by deformation and degradation: laboratory testing and numerical modeling, Int. J. Geomech. 20 (1) (2020) 04019138-1-04019138-14.
[8] B. Indraratna, S. Nimbalkar, Stress-strain degradation response of railway ballast stabilized with geosynthetics, J. Geotech. Geoenviron. Eng. 139 (5) (2013) 684–700.
[9] V.V. Krylov, Effects of track properties on ground vibrations generated by high-speed trains, Acta Acust. United Acust. 84 (1) (1998) 78–90.
[10] L. Auersch, Simple and fast prediction of train-induced track forces, ground and building vibrations, Rail. Eng. Sci. 28 (2020) 232–250.
[11] S. Ouakka, O. Verlinden, G. Kouroussis, Railway ground vibration and mitigation measures: benchmarking of best practices, Rail. Eng. Sci. 30 (2022) 1–22.
[12] A. Najibi, G.Q. Jing, Two dimensional stress wave propagation analysis of infinite 2D-FGM hollow cylinder, Waves Random Complex Media 31 (2021) 1–18.

[13] A.G. Correia, J. Cunha, J. Marcelino, L. Caldeira, J. Varandas, Z. Dimitrovová, Dynamic analysis of rail track for high-speed trains.2D approach. 5thInt Worksop On Application of Computational Mechanics On Geotechnical Eng, Taylor & Francis Group, Portugal, 2007, pp. 1–14.
[14] G. Giner, A.R. Alvarez, C.J.L. García-MorenoSS-C, Dynamic modelling of high-speed ballasted railway tracks: analysis of the behaviour, Transp. Res. Procedia 18 (2016) 357–365.
[15] Q. Sun, B. Indraratna, J. Grant, Numerical simulation of the dynamic response of ballasted track overlying a tire-reinforced capping layer, Front. Built Environ. 6 (2020) 6. –6.
[16] L. Hall, Simulations and analyses of train-induced ground vibrations in finite element models, Soil Dyn. Earthq. Eng. 23 (5) (2003) 403–413.
[17] K. Nguyen, J.M. Goicolea, F. Galbadon, Comparison of dynamic effects of high-speed traffic load on ballasted track using a simplified two-dimensional and full three-dimensional model, Proc. Inst. Mech. Eng. 228 (2) (2014) 128–142.
[18] K.G. Babu, C. Sujatha, Track modulus analysis of railway track system using finite element model, J. Vib. Control 16 (10) (2010) 1559–1574.
[19] Q. Fu, C. Zheng, Three-dimensional dynamic analyses of track-embankment-ground system subjected to high-speed train loads, Sci. World J, 2014 (2014) 924592.
[20] S. Likitlersuang, P. Pholkainuwatra, T. Chompoorat, S. Keawsawasvong, Numerical modelling of rail- way embankments for high-speed train constructed on soft soil, J. Geo Eng. 13 (3) (2018) 149–159.
[21] M.A. Sayeed, M.A. Shahin, Three-dimensional numerical modelling of ballasted railway track foundations for high-speed trains with special reference to critical speed, Transp. Geotech. 6 (2016) 55–65.
[22] G. Kumaran, D. Menon, K.K. Nair, Dynamic studies of rail track sleepers in a track structure system, J. Sound Vib. 268 (3) (2003) 485–501.
[23] M.P.N. Burrow, D. Bowness, G.S. Ghataora, A comparison of railway track foundation design methods, Proc. Inst. Mech. Eng. F J. Rail Rapid Transit 221 (1) (2007) 1–12.
[24] D. Li, E.T. Selig, Method for railroad track foundation design. I: development, J. Geotech. Geoenviron. Eng. 124 (4) (1998) 4. –4.
[25] Joint feasibility study for Mumbai-Ahmedabad High-Speed Railway, Corridor, 5, (2015) 4–28.
[26] Specifications for Railway Formation, Indian Railways, RDSO/2018/GE, 2018.
[27] Detailed Project Report, Kochi Metro Project, Kerala, 5 (5) (2011) 31–40.
[28] B.T. Jose, A. Sridharan, B.M. Abraham, A study of geotechnical properties of Cochin marine clays, Mar. Georesources Geotechnol. 7 (3) (1988) 189–209.
[29] R. Sundaram, S. Gupta, A. Varghese, Piles through Soft clay for a metro project, in: Proceedings of the DFI India 2016, Calcutta, 2016.
[30] J.E Bowles, Foundation Analysis and Design, 3rd edition, McGraw-Hill, New York, 1982.
[31] B.M. Das, Advanced Soil Mechanics, McGraw-Hill Book Company, New York, 1983.
[32] M. Farzi, S. Zadeh, A. Determination of relationship between standard penetration test and geotechnical parameters in Ahwaz soil, Geomech. Geoeng. 16 (6) (2021) 421–433.
[33] A.J. Lutenegger, D.J. Degroot, Settlement of Shallow Foundations On Granular Soils, University of Massachusetts Transportation Center, 1995.
[34] E. Sayed, A.A.E. Kasaby, Estimation of guide values for the modulus of elasticity of soil, Bull. Fac. Eng. Assiut Univ. 19 (1) (1991) 1–7.
[35] R. Kumar, K. Bhargava, D. Choudhury, Estimation of engineering properties of soils from field SPT using random number generation, INAE Lett. 1 (3–4) (2016) 77–84.
[36] K.S. Beena, M.N. Sandeep, Numerical modelling of Rayleigh wave in homogeneous soil medium in undamped condition, Indian Geotech. J. 52 (2022) 55–69.
[37] S.L. Kramer. Geotechnical Earthquake Engineering, Pearson Education India, 1996.
[38] P. Anbazhagan, B. Indraratna, G. Amarajeevi, Characterization of clean and fouled rail track ballast subsurface using seismic surface survey method: model and field studies, J. Test. Eval. 39 (5) (2011) 831–841.
[39] G. Miller, H. Pursey, E.C. Bullard, On the partition of energy between elastic waves in a semi-infinite solid, Proc. R. Soc. Lond. A. Math. Phys. Sci. 233 (1955) 55–69.
[40] G.J. Rix, C.G. Lai, M.C. Orozco, G.L. Hebeler, V. Roma, Recent advances in surface wave methods for geotechnical site characterization, Proc. Int. Conf. Soil Mech. Geotech. Eng. 1 (2001) 499–502.
[41] R. Luna, H. Jadi, Determination of dynamic soil properties using geophysical methods, in: Proceedings of the first international conference on the application of geophysical and NDT methodologies to transportation facilities and infrastructure, 2000, pp. 1–15.
[42] T. Kokusho, Innovative Earthquake Soil Dynamics, CRC Press, 2017.
[43] M.E. Raghunandan, Effect of soil layering on the ground response parameters: a parametric study, Nat. Hazards 63 (2) (2012) 1115–1128.
[44] R. Ferrara, G. Leonardi, F.A. Jourdan, Two-dimensional numerical model to analyze the critical velocity of high-speed infrastructure, in: Proceedings of the Fourteenth International Conference on Civil, Structural and Environmental Engineering Computing, Calgiari, Italy, 2013.
[45] P. Mandhaniya, S. Chandra, J.T. Shahu, Finite element analysis of moving load on ballastless rail track, Geotech. Charact. Model. 85 (2020) 839–848.
[46] Deutsches Institutfür Normung, DIN4150-2: Structural Vibrations Part 2: Human exposure to vibration in buildings, 1999.
[47] Transit Noise and Vibration Impact Assessment Manual, Federal Transit Administration, US Department of Transportation FTA report no0123 2018.
[48] A. Tucho, B. Indraratna, T. Ngo, Stress-deformation analysis of rail substructure under moving wheel load, Transp. Geotech. 36 (2022), 100805.